



Pre-chamber combustion system for heavy-duty engines for operating dual fuel and diesel modes

Jisoo Shin^a, Jonghui Choi^a, Jaeyeob Seo^b, Sungwook Park^{c,*}

^a Department of Mechanical Convergence Engineering, Graduate School of Hanyang University, Seoul 04763, Republic of Korea

^b Advanced Propulsion System Research Department, Korea Shipbuilding and Offshore Engineering, Seoul 03058, Republic of Korea

^c School of Mechanical Engineering, Hanyang University, Seoul 04763, Republic of Korea

ARTICLE INFO

Keywords:

Heavy-duty engine
Pre-chamber
Indirect injection
CFD
Marine vehicle

ABSTRACT

With the increase in heavy-duty engines, an enhanced combustion concept is necessary to meet stringent environmental regulations. Pre-chamber combustion systems can be used to improve combustion stability and emissions, and their design parameters are important because they affect the jet properties and engine performance. Therefore, this study investigates the combustion and emission characteristics of a pre-chamber combustion system for heavy-duty engines using a CFD program to determine the optimal design for engine performance. The simulation was conducted with an engine speed of 720 rpm and a 100% load condition for both dual fuel and diesel-only operation modes. Results indicate that the optimal pre-chamber nozzle design parameters include a hole diameter of 2.4 cm, 4 holes, and a direction angle of 60 deg. Compared with a conventional engine, the gross IMEP for an engine with a pre-chamber combustion system increased up to 0.8%, and the THC emissions was significantly reduced by preventing methane slip in dual-fuel mode. Additionally, NOx production was reduced by 50% in diesel mode. However, the NOx in dual-fuel mode and the soot in diesel mode were deteriorated. Therefore, engine operating strategies for pre-chamber combustion systems should be investigated as future work.

1. Introduction

With the increasing volume of global transportation, concerns about emissions from the transport sector [1], which includes a large portion of heavy-duty engine for marine vehicles, continue to increase. In response to environmental issues around the world, various combustion strategies associated with fuels and engine design have been developed for use in internal combustion engines [2]. Saiteja and Ashok [3] highlighted the advantage of biofuels to replace fossil fuels and reduce exhaust emissions with conventional engines. Furthermore, they investigated the homogeneous charge preparation technique of a homogeneous charge compression ignition (HCCI) engine powered by biofuels. The use of gaseous fuel in addition to liquid diesel in dual-fuel mode is another method to reduce the emissions of diesel engines [4]. Therefore, considering dual-fuel mode for diesel engines may help address emission concerns. Regarding engine design, a pre-chamber ignition system can improve inflammability and thereby ensure stable combustion in gas engines with lean conditions [5].

In addition, indirect injection based on the Comet Mk pre-chamber

combustion system has been developed for diesel engines [6,7]. Salahi et al., [8] conducted simulations for the Comet Mk combustion pre-chamber to investigate the reactivity controlled compression ignition (RCCI) combustion strategy in an engine fueled by natural gas and diesel. They found that introducing the active fuel in a thermally insulated pre-chamber extended the operating range under a lower intake-air temperature for both low and high loads. Esfahanian et al., [9] also investigated the effects of two combustion concepts, homogeneous charge compression ignition and premixed charge compression ignition, in a pre-chamber, dual-fuel engine system to improve the combustion efficiency and emissions.

Huang et al., [10] studied the application of an indirect injection system, which is a type of pre-chamber system, to a diesel engine. The pre-chamber system slowed the combustion process in the diesel engine, decreasing the peak combustion temperature. Therefore, it reduced the brake thermal efficiency but drastically reduced NOx emissions. Iwazaki et al., [11] found that two-stage injection in an indirect injection system improved engine fuel consumption by 20% at a certain injection timing.

Thus, in previous studies, applying pre-chamber systems to gas and diesel engines produced certain thermal efficiency advantages in dual-

* Corresponding author at: School of Mechanical Engineering, Hanyang University, 222 Wangsimni-ro, Seongdong-gu, Seoul 04763, Republic of Korea.

E-mail address: parks@hanyang.ac.kr (S. Park).

Nomenclature			
ΔP	Pressure difference between pre-chamber and main chamber	$S_{l,ref}$	Reference laminar flame speed
ε	Turbulent dissipation	S_t	Turbulent flame speed
λ	Air-fuel equivalence ratio	T_u	Unburned temperature
ρ_u	Unburned density	$T_{u,ref}$	Reference unburned temperature
Y_{dil}	Mass fraction of dilution species	$V_{chamber@TDC}$	Volume of combustion chamber at TDC
ϕ	Equivalence ratio	$V_{pre-chamber}$	Volume of pre-chamber
D_t	Turbulent diffusion		
k	Turbulent kinetic energy	Abbreviations	
P	Pressure	HCCI	Homogeneous Charge Compression Ignition
P_{ref}	Reference pressure	RCCI	Reactivity Controlled Compression Ignition
S_l	Laminar flame speed	THC	Total Hydrocarbon
		CFD	Computational Fluid Dynamics
		LHV	Lower Heating Value
		IMEP	Indicated Mean Effective Pressure

fuel engines and NOx emission advantages in diesel engines.

It is necessary to understand the influence of pre-chamber design parameters because the jet characteristics vary with these parameters, which thus play an important role in the combustion process, further affecting the emissions. Gentz et al., [12] studied how the pre-chamber orifice diameter affected a turbulent jet ignition system fueled by propane with a spark plug in the pre-chamber. Based on the optical image and combustion characteristics, they determined the relationships between the jet velocity and structure, the combustion process, and different pre-chamber orifices. When the operation was lean (λ greater than 1.25), a more vigorous jet with greater initial jet penetration was required. Shah et al., [13] investigated the effect of pre-chamber volume and nozzle diameter on a natural gas engine equipped with a spark plug. Using a single nozzle hole direction angle, they analyzed the flame development and combustion characteristics of three pre-chamber shapes with different volumes, nozzle hole diameters, and throat area ratios. In a diesel engine pre-chamber system, Nishida et al., [7] found that the nozzle hole size influenced the flame jet and turbulence, playing a major role in determining the brake mean effective pressure, smoke, and NOx.

To utilize the advantages of a pre-chamber system in a heavy-duty engine for marine vehicles that have large displacements and consume a large amount of fuel, it is necessary to optimize the pre-chamber system for a heavy-duty engine. Because there are few studies on pre-chamber systems in heavy-duty engines, additional study is needed. To introduce a pre-chamber system to a heavy-duty engine capable of both dual fuel and diesel-only operation modes, the combustion process must be investigated first, followed by the emissions characteristics in the pre-chamber combustion system. The pre-chamber design can then be analyzed based on these results. The pre-chamber design parameters that play an important role in the combustion process, such as the pre-chamber nozzle hole area and jet targeting, should be optimized while considering both dual fuel and diesel-only operation modes.

Therefore, in this study, the combustion process of a heavy-duty engine with an applied pre-chamber system was analyzed in both dual fuel and diesel-only operation modes. Then, the influence of the pre-chamber nozzle hole diameter, number, and direction angle was investigated in both operational modes. In dual fuel mode operation fueled by diesel (as a high reactivity fuel) and methane (as a low reactivity fuel), the efficiency and THC (total hydrocarbon) resulting from methane slip is important, in addition to NOx emissions. Therefore, the gross indicated mean effective pressure (IMEP), NOx, and THC were used to evaluate the effects of the aforementioned parameters. In diesel mode operation, soot formation from incomplete combustion and NOx were used for the evaluation. This study conducted CFD (computational fluid dynamics) simulations using CONVERGE v2.4 software.

2. Computational methodology

2.1. Numerical model

To simulate the combustion process in the cylinder of a heavy-duty engine, the software CONVERGE v2.4 was used. The turbulence flow was modeled using the RNG k- ε turbulence model with the Reynolds-averaged Navier-Stokes equation [14,15]. The diesel spray break-up process was simulated using the Kelvin Helmholtz-Rayleigh Taylor break-up model [16], which is generally used to model a high-pressure spray break-up process. N-tetradecane ($C_{14}H_{30}$) was used as a surrogate fuel for the physical properties of liquid diesel, and the Frossling model was used to simulate fuel evaporation.

To simulate the dual fuel combustion process with a micro-pilot diesel injection, the combined combustion model shown in Fig. 1 was used.

The diesel pilot spray ignition was modeled by the SAGE detailed chemistry model in CONVERGE using n-heptane (42 species and 168 reactions) [17] as the surrogate for diesel fuel during the combustion process. No additional methane combustion mechanism was required because the n-heptane combustion mechanism includes the methane oxidation process. In the SAGE model, each chemical reaction rate has an Arrhenius equation form. This approach assumes that each computational cell is homogeneous. The chemistry model predicts the ignition delay, early flame kernel formation location, and flame propagation speed of diesel diffusion combustion.

The premixed combustion was modeled using the level-set G-equation approach to simulate premixed flame propagation [18]. The scalar variable G is the scalar distance function between the immediate position and the mean flame front. A $G = 0$ surface indicates that the flame front is at the immediate position. The G-equation model for turbulent premixed combustion is based on the advanced form of the Favre mean variance equation for G [19]. To track the turbulent flame front by solving for the mean of G, Eqs. (1) and (2) were used where S_t is the turbulent flame speed, ρ_u is the unburned density, k is the turbulent kinetic energy, D_t is the turbulent diffusion and ε is the turbulent dissipation.

$$\frac{\partial \rho G}{\partial t} + \frac{\partial \rho u_i G}{\partial x_i} = -\rho D_t \kappa \left| \frac{\partial G}{\partial x_i} \right| + \rho_u S_t \left| \frac{\partial G}{\partial x_i} \right| \quad (1)$$

$$\frac{\partial \rho G''^2}{\partial t} + \frac{\partial \rho u_i G''^2}{\partial x_i} = \frac{\partial}{\partial x_i} \left(\rho D_t \frac{\partial G''^2}{\partial x_i} \right) + 2\rho D_t \frac{\partial G}{\partial x_i} \frac{\partial G}{\partial x_i} - c_s \rho G''^2 \frac{\varepsilon}{k} \quad (2)$$

For the calculation of the laminar flame speed of methane, the Gulder correlation [20] was used based on the following Eqs. (3)-(6), where T_u is the unburned temperature, $T_{u,ref}$ is the reference unburned temperature, P is the pressure, P_{ref} is the reference pressure, Y_{dil} is the

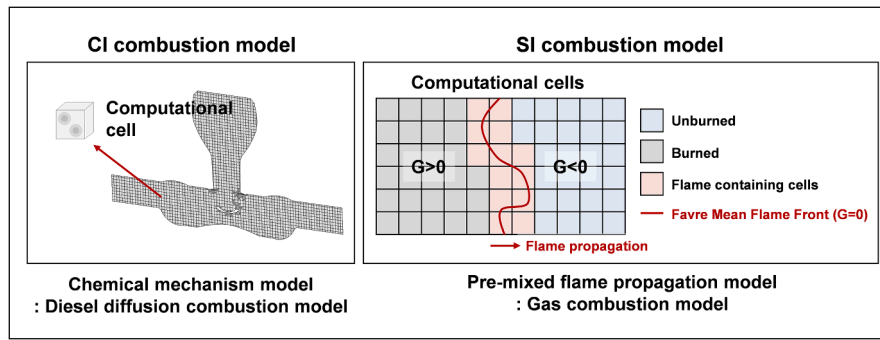


Fig. 1. Combined combustion model to simulate a dual fuel combustion process using diesel injection for the ignition.

mass fraction of dilution species, and ϕ is the equivalence ratio.

$$S_{i,ref} = \omega \phi^n \exp[-\xi(\phi - 1.075)^2] \quad (3)$$

$$S_i = S_{i,ref} (T_u/T_{u,ref})^\gamma (P/P_{ref})^\beta (1 - 2.1Y_{dil}) \quad (4)$$

$$\gamma = a_T + m_T(\phi - 1) \quad (5)$$

$$\beta = a_p + m_T \phi^{3.51} \quad (6)$$

The model constants for these equations which were modified during the validation process are presented in Table 1.

At the start of the calculation, the G value was not declared in the computational domain. For conventional gasoline and gas engine simulations, the source of G was valued directly, or the initial kernel size for g-equation propagation was set. In this study, when the cell temperature reached 1600 K, the g value was initialized, and flame propagation began. Combining the g-equation with the detailed chemistry model in this way predicted the ignition delay and ignition point through the chemical reaction mechanism, which allowed the flame propagation velocity to be predicted through the g-equation model.

The extended Zel'dovich model [21] was used to predict NOx emissions. Most of the NOx from the diesel engine combustion is thermal NOx, so only thermal NOx was considered in this study. The Hiroyasu soot model was applied using total hydrocarbons as the soot formation precursor. This model is empirical and divides the soot formation process into just two processes: formation and oxidation [22]. The formation and oxidation masses are determined by the in-cylinder pressure, temperature, concentration of the soot precursor, and oxygen partial pressure.

2.2. Validation of combined combustion model

The combined combustion model was validated based on experimental results of a conventional heavy-duty engine with bore-stroke ratio of 0.875. The validation was conducted at an engine speed of 720 rpm. In dual-fuel mode, the intake pressure was 1.46 bar at 50% load and 2.78 bar at 100% load, and in diesel fuel operation mode, the intake pressure was 1.78 bar at 50% load and 3.3 bar at 100% load. The engine load conditions were experimentally determined according to

the IMEP. The in-cylinder pressure behavior and apparent heat release rate comparison between experimental and simulated results are presented in Fig. 2. The results show a reasonable trend with increasing engine load in dual fuel mode and diesel mode operations.

The errors in the simulation results were evaluated for the in-cylinder maximum pressure and timing at which the in-cylinder pressure had a maximum value as shown in Table 2. Under dual fuel operation conditions, the in-cylinder maximum pressure error was 10.4 % at 100% load. This affected the high-combustion variation during dual-fuel combustion compared with diesel combustion. For the error in the maximum in-cylinder pressure timing, only a maximum error of 1.2 deg appears in dual-fuel mode. Additionally, the errors in the in-cylinder maximum pressure and its timing were reasonably low in diesel operation mode. Therefore, these results indicate that the simulation models for dual-fuel mode and diesel mode can sufficiently reflect experimental results.

2.3. Simulation conditions

During dual fuel mode operation, the engine was operated with methane as the primary fuel and diesel as the secondary injected fuel. The overall lambda in the cylinder was set to 1.87, and the proportion of fuels based on the LHV (lower heating value) was 99.5% and 0.5% for natural gas and diesel, respectively. The intake pressure was 2.78 bar. During diesel mode operation, the overall lambda in the cylinder was set to 2.14. The diesel fuel was injected with a pilot with the main injection ratio of 0.9:99.1. The intake pressure was 3.3 bar in diesel mode.

To investigate the combustion characteristics of the pre-chamber combustion system, the engine operating conditions listed in Table 3 were used. These operating conditions were based on experiment results of a conventional heavy-duty engine operating at 100% load. However, based on the simulation results of the combustion characteristics of the pre-chamber combustion system, the injection timings were adjusted. In dual fuel mode operation, the injection timing was delayed compared with that in a conventional gas engine due to the shorter combustion duration of the pre-chamber combustion system. In contrast, in diesel mode operation, the injection timing was accelerated compared with that in conventional diesel operation because of the longer combustion duration that resulted from using the pre-chamber combustion system.

With a pre-chamber combustion system, the combustion process occurs in two stages with the first stage occurring in the pre-chamber and the second stage occurring in the main chamber. The pre-chamber and main chamber are connected by a nozzle; thus, the pre-chamber nozzle hole layout is important in determining the flame propagation and combustion phase from the pre-chamber to the main chamber. Therefore, in this study, the pre-chamber nozzle design parameters that pertain to flame propagation were selected as shown in Fig. 3 and Table 4. With the compression ratio fixed, the influence of the pre-chamber nozzle design was investigated for both dual fuel and diesel operation modes.

Table 1

Model constants for the Gulder correlation.

ω	0.422
η	-0.2
ξ	1.5
γ	2.0
β	-0.1
m_T	-0.8
m_p	0.15
Y_{dil}	0.0

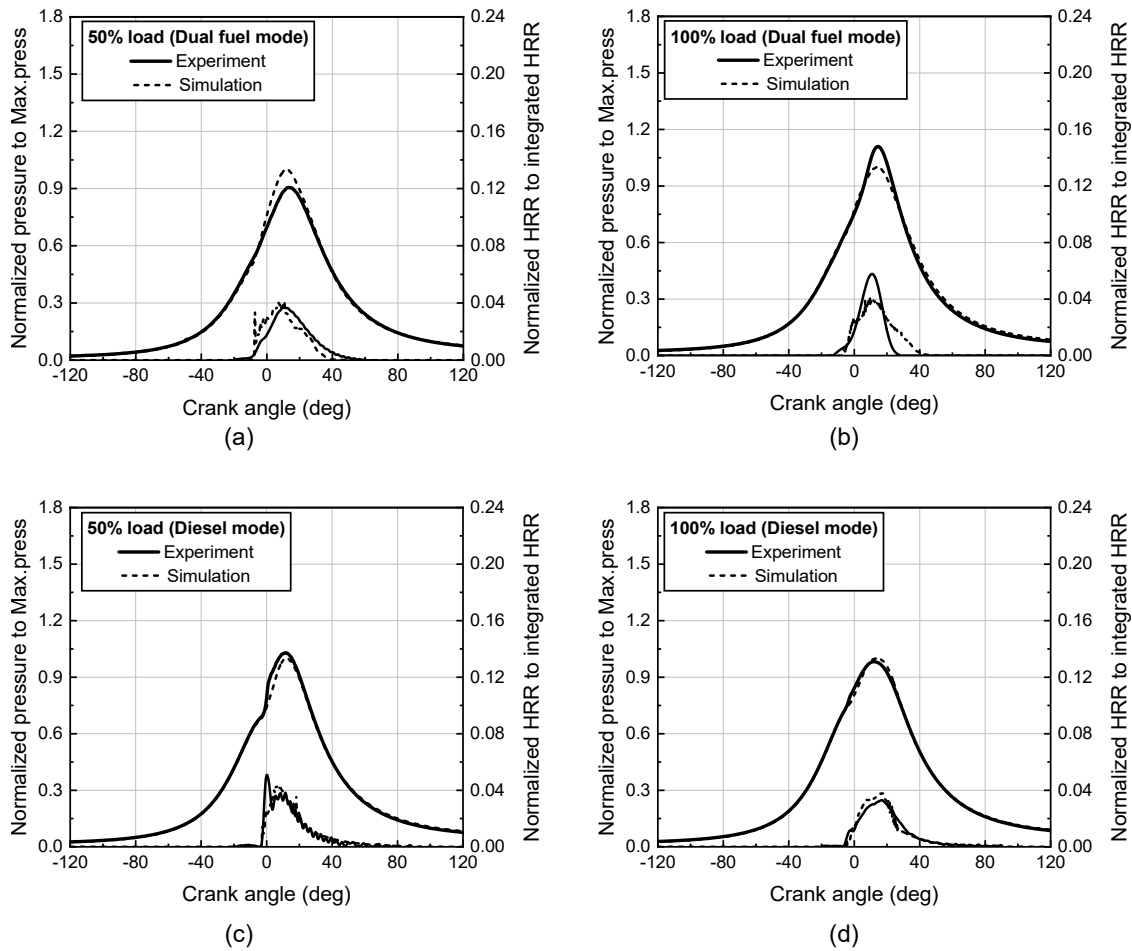


Fig. 2. Combustion model validation results at (a) 50% load and (b) 100% load in dual fuel mode operation, and at (c) 50% load and (d) 100% load in diesel mode operation.

Table 2
Combustion simulation errors.

Experimental and simulation conditions	P_{max} error	P_{max} timing error	
Dual-fuel mode	50% load	10.0 %	1.2 deg
	100% load	10.4 %	0.4 deg
Diesel mode	50% load	2.9 %	0.0 deg
	100% load	1.7 %	2.1 deg

3. Results and discussion

3.1. Combustion process in the pre-chamber combustion system

The combustion process under dual fuel mode operation with diesel micro-pilot injection and without a pre-chamber is presented in [23]. In dual fuel mode operation, unlike in diesel mode operation, there is little or no controlled-mixing region; instead, flame propagation combustion occurs [24]. However, in an engine system with a pre-chamber, the combustion step inside the pre-chamber is added because the pre-chamber has an additional volume that must be distinguished from the main chamber. The combustion process of an engine system with a pre-chamber is illustrated in Fig. 4. When micro-pilot diesel fuel is injected into the pre-chamber, the gas fuel in the pre-chamber burns first

Table 3
Engine operating conditions.

Operation mode		
Dual fuel mode operation	Engine speed	720 rpm
	Lambda (λ)	1.87
	Injector nozzle hole number	4
	Injector nozzle hole diameter	0.25 mm
	Injection angle	17°
	Injection timing	-8 CAD
	Injection duration	3.15 deg
	Micro pilot diesel quantity	0.5% of total LHV
	Gas fuel species	Methane (CH ₄)
	Diesel mode operation	Engine speed
Lambda (λ)		2.14
Injector nozzle hole number		4 (pilot), 12 (main)
Injector nozzle hole diameter		0.25 mm (pilot), 0.48 mm (main)
Injection angle		17° (pilot), 17° (main)
Injection timing		-11 CAD (pilot), -9 CAD (main)
Injection duration		4.9 deg (pilot), 25.8 deg (main)
Diesel injection quantity ratio (pilot : main)		0.9% : 99.1%

(after the ignition delay). During this period, the heat release rate is increased slightly (Fig. 4(a)). After, the flame jet from the pre-chamber propagates to the main chamber, and the heat release rate rises due to the fast flame jet formed by the pre-chamber (Fig. 4(b)). The flame propagation by the flame jet is faster than that without a pre-chamber

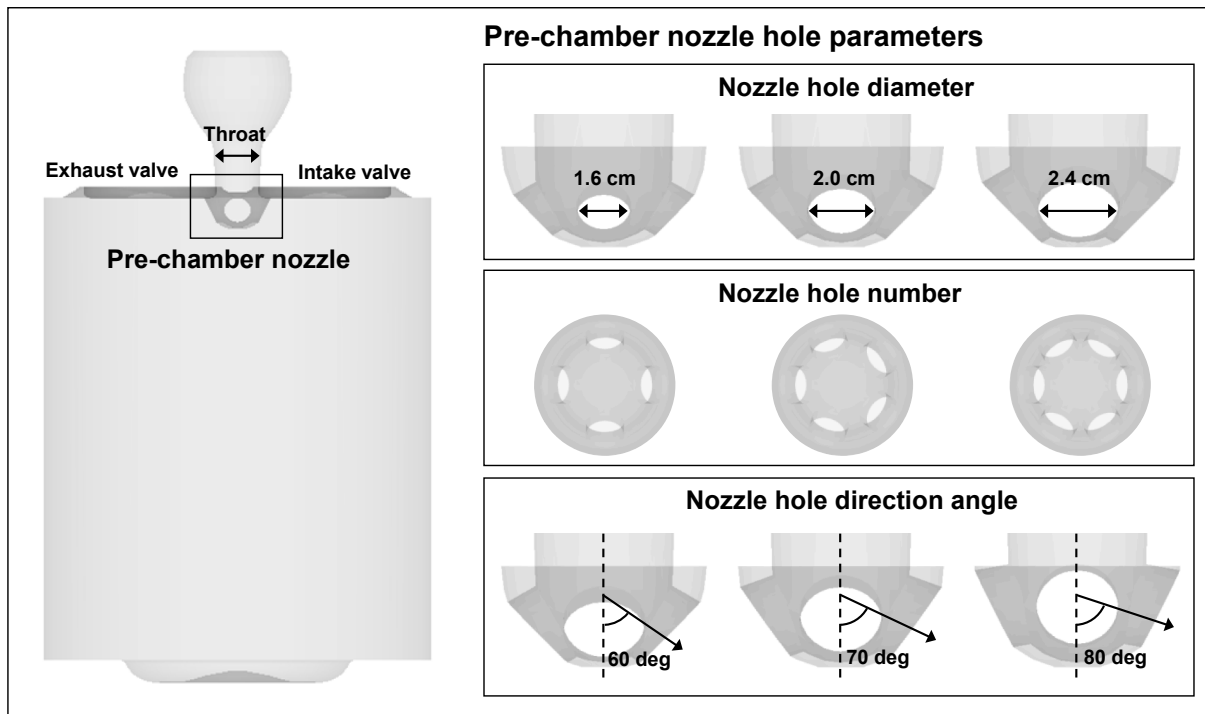


Fig. 3. Computational domain and geometry for the simulation parameters.

Table 4
Simulation conditions for the pre-chamber combustion system.

Pre-chamber volume	525 cm ³		
Volume ratio ($V_{\text{pre-chamber}}/V_{\text{chamber@TDC}}$)	0.17		
Throat area	14.6 cm ²		
Pre-chamber nozzle hole diameter	1.6 cm, 2.0 cm, 2.4 cm	1.6 cm	2.4 cm
Pre-chamber nozzle hole number	4	4, 5, 6	4
Pre-chamber nozzle hole direction angle	60 deg	60 deg	60 deg, 70 deg, 80 deg

because of the high jet velocity. When the flame is sufficiently developed and the flame area increases, the end gas burns rapidly, producing a rapid increase in the heat release rate (Fig. 4(c)). This is similar to pre-mixed combustion, which is promising for high efficiency [25] because flame propagation and auto ignition of the end gas occur.

Conventional diesel combustion generally consists of four phases: ignition delay, premixed combustion, mixing controlled combustion, and late burning [26]. In a pre-chamber combustion system, the limitation of oxygen in the pre-chamber slows the heat release rate during premixed combustion, as shown in Fig. 5(d). After the diesel fuel vapor and flame are ejected into the main chamber (Fig. 5(e)), the fuel vapor and air mixing process takes place in the main chamber. In this mixing controlled phase, the mixing performance is affected by the pre-chamber nozzle hole layout. When the fuel vapor supply from the pre-chamber is stopped, combustion goes through the late burning phase as the rest of the fuel burns continually and the heat release rate drops.

In diesel mode operation, the soot formation process in the main chamber is explained by a conceptual model in [27]. Unlike in a direct-injection diesel combustion system, the fuel ejected from the pre-chamber is in a vapor state, but the spatial characteristics of soot formation and flame have the same form. The fuel/air mixture distributed near the pre-chamber nozzle is rich, so the products of rich combustion

such as soot are formed in this region (~1600 K). Flame diffusion (~2700 K) occurs between the rich fuel/air mixture area and air and is the source of the high OH radicals that play an important role in soot oxidation [28]. Thus, soot oxidation occurs mainly in the flame diffusion area, as shown in Fig. 6. Because of the high-temperature region near the flame diffusion, thermal NOx production is expected only around the flame jet periphery on the lean side of the flame diffusion [27]. Therefore, the flame structure and combustion temperature should also be investigated to understand the emissions.

For combustion process in pre-chamber combustion system, the flame jet properties which mainly affected by the pre-chamber nozzle hole designs are important in both dual-fuel and diesel modes. Therefore, the combustion and emission characteristics for the pre-chamber nozzle hole design were investigated in following sections.

3.2. Influence of the pre-chamber nozzle hole diameter

As the pre-chamber nozzle hole diameter increased, the pressure difference between the pre-chamber and main chamber during compression decreased (Fig. 7). This is because when the number of nozzle holes is held constant, a larger pre-chamber nozzle hole size equals a larger nozzle hole area, and a larger nozzle hole area improves the pressure response of the pre-chamber to pressure changes in the main chamber. Similarly, the pressure difference between the pre-chamber and the main chamber decreased as the nozzle hole diameter increased when the pressure rose in the pre-chamber after diesel injection.

Combustion phasing and combustion duration directly affect the thermal efficiency [29] and can be used to assess the combustion process of an internal combustion engine [30]. They are thus important parameters for understanding combustion characteristics, along with the in-cylinder pressure and heat release rate.

In Fig. 8, the combustion characteristics with different pre-chamber nozzle hole diameters are presented. As the pre-chamber nozzle hole diameter increased, the flame jet velocity from the pre-chamber decreased, reducing the pressure difference between the pre-chamber

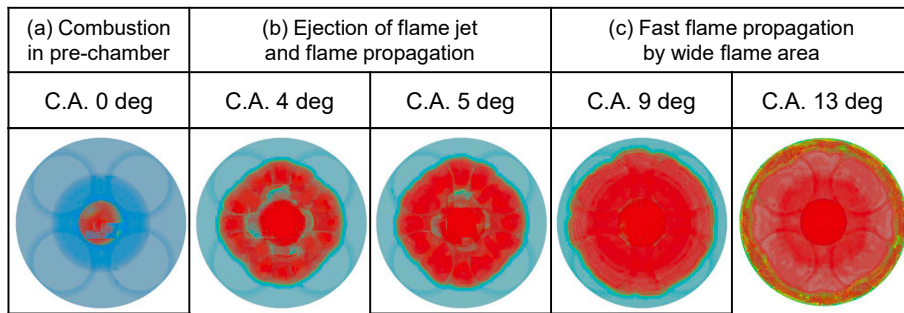
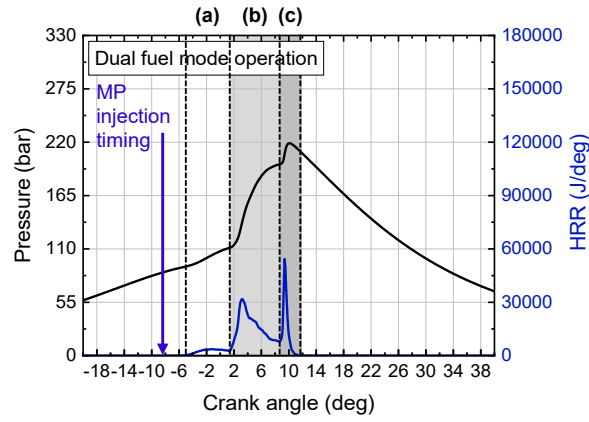


Fig. 4. Combustion process of a heavy-duty engine with a pre-chamber in dual fuel mode operation.

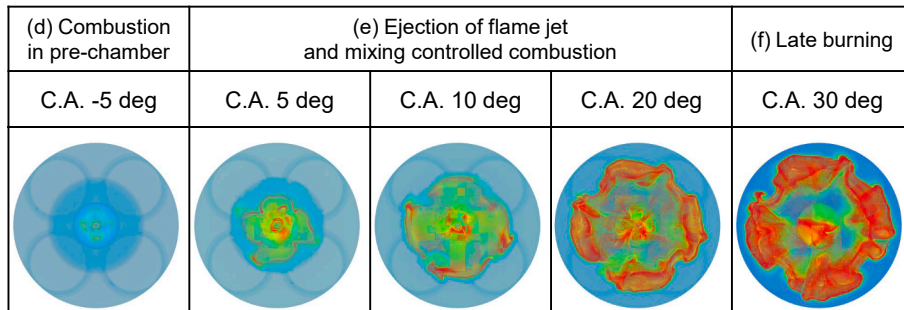
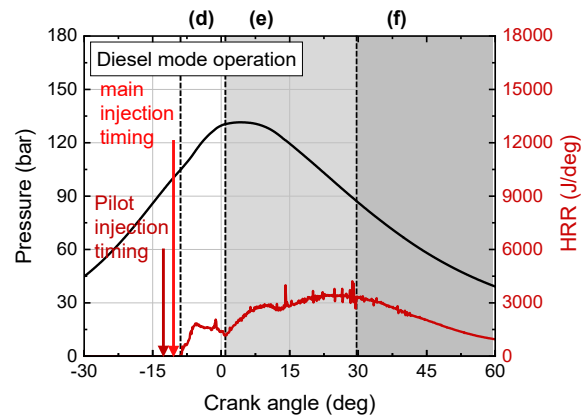


Fig. 5. Combustion process of a heavy-duty engine with a pre-chamber in diesel mode operation.

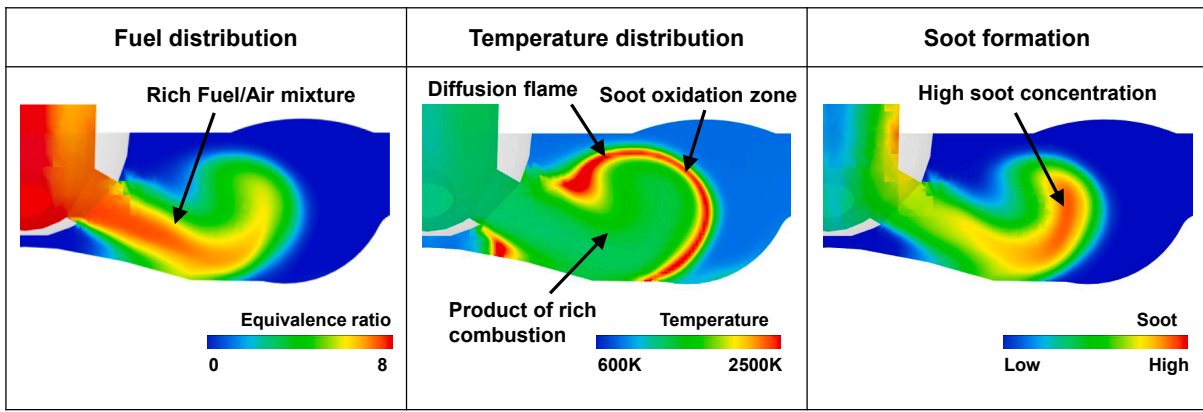


Fig. 6. Jet properties in diesel operation mode with a pre-chamber.

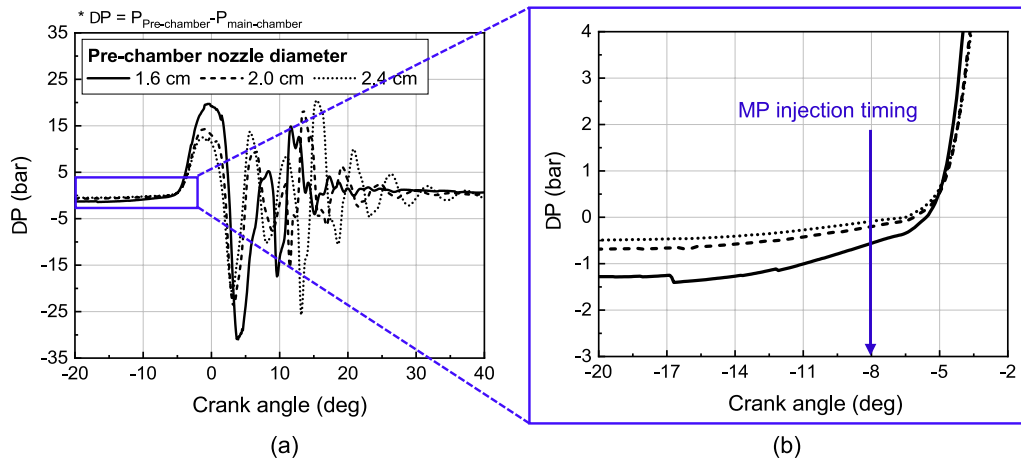


Fig. 7. Pressure difference between the pre-chamber and main chamber based on the pre-chamber nozzle hole diameter in dual fuel mode operation (a) from C.A. -20 deg to C.A. 40 deg, (b) enlarged.

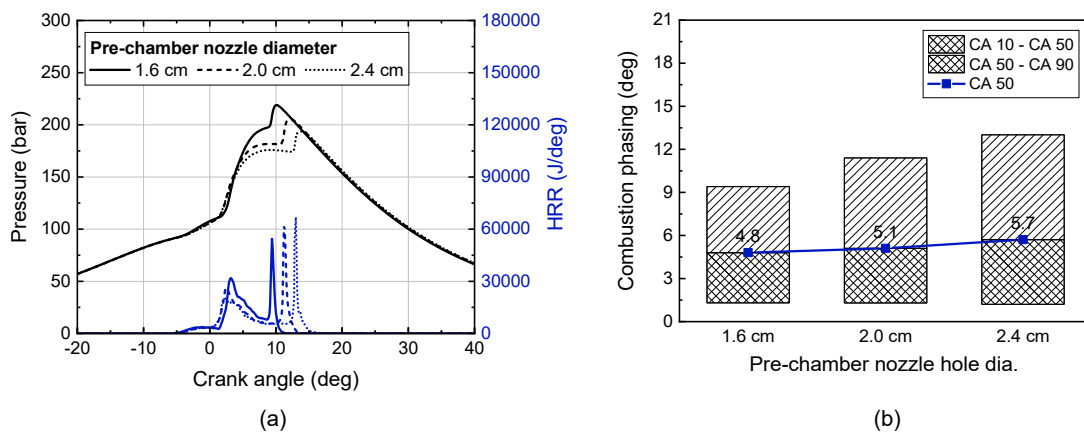


Fig. 8. (a) In-cylinder pressure and heat release rate. (b) Combustion phasing based on the pre-chamber nozzle hole diameter in dual fuel mode operation.

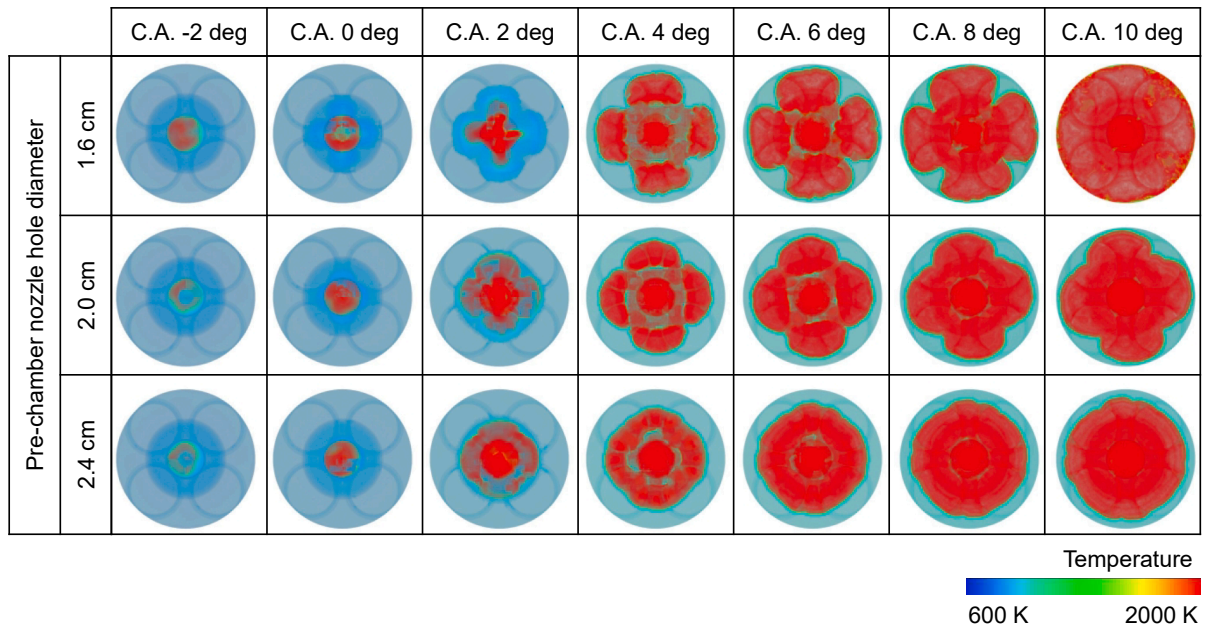


Fig. 9. Flame propagation based on the pre-chamber nozzle hole diameter in dual fuel mode operation.

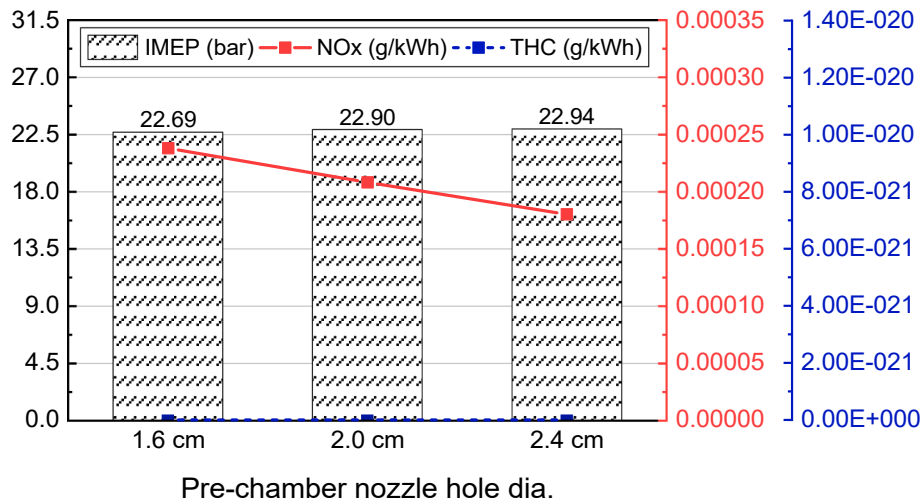


Fig. 10. Gross IMEP and emissions based on the pre-chamber nozzle hole diameter in dual fuel mode operation.

and the main chamber. Therefore, the combustion phasing (CA50) and peak pressure timing were retarded as the pre-chamber nozzle hole diameter increased. The slower flame propagation that occurred as the nozzle hole diameter increased caused the combustion duration to last longer (CA10–CA90), decreasing the peak pressure.

Fig. 9 shows how the pre-chamber nozzle hole diameter influences the flame structure. As the pre-chamber nozzle hole size increased, the flame jet diverged into a wider angle and had more possibility of merging with the flame jets from other nozzle outlets. Because the flame propagation slowed as the pre-chamber nozzle hole diameter increased, the high-temperature flame region near the peak pressure timing became decreased. Therefore, the peak pressure decreased as the pre-chamber nozzle hole diameter increased.

To evaluate the combustion efficiency and emissions in dual fuel mode operation, the gross IMEP, NOx, and THC were calculated, as shown in Fig. 10. Because of the longer combustion duration caused by larger pre-chamber nozzle hole diameters (Fig. 8), the positive work with a nozzle hole diameter of 2.4 cm was greater than that with a

smaller nozzle hole diameter, increasing the gross IMEP by up to 1.1%.

The decrease in peak pressure of the larger pre-chamber nozzle hole reduced NOx emissions. Furthermore, the fast and even flame propagation reduced methane slip, as indicated by the very small amount of THC generated.

In diesel mode operation, understanding the combustion process of a pre-chamber combustion system should consider not only the jet velocity but also the diesel fuel vapor supply to the main chamber. The fuel vapor distributions are determined by the jet velocity and jet angle. A higher jet velocity allows the diesel vapor to penetrate faster in the radial direction. As a result, the fuel tends to be distributed more widely in the radial direction. However, a wider jet angle or increased merging of jets from multiple nozzle holes causes the fuel vapor to be distributed in a wider area in the angular direction. The most uniform fuel distribution occurred when the jets from each nozzle outlet merged when the nozzle hole diameter was 2.4 cm. However, when the jets from each nozzle remained separate, the fuel was more evenly and widely distributed at a higher jet velocity (Fig. 11(a)).

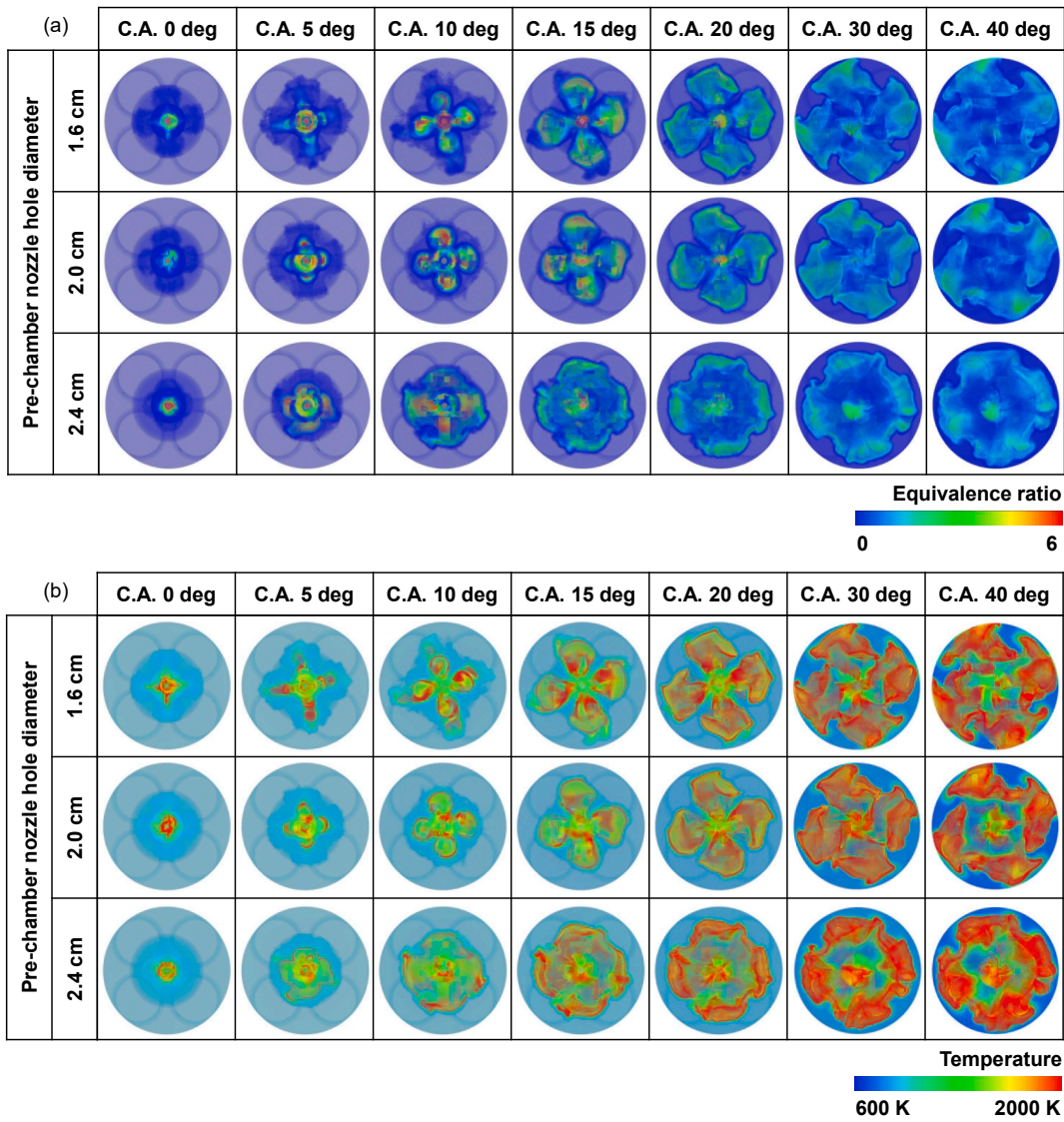


Fig. 11. (a) Diesel vapor and (b) flame propagation based on the pre-chamber nozzle hole diameter in diesel mode operation.

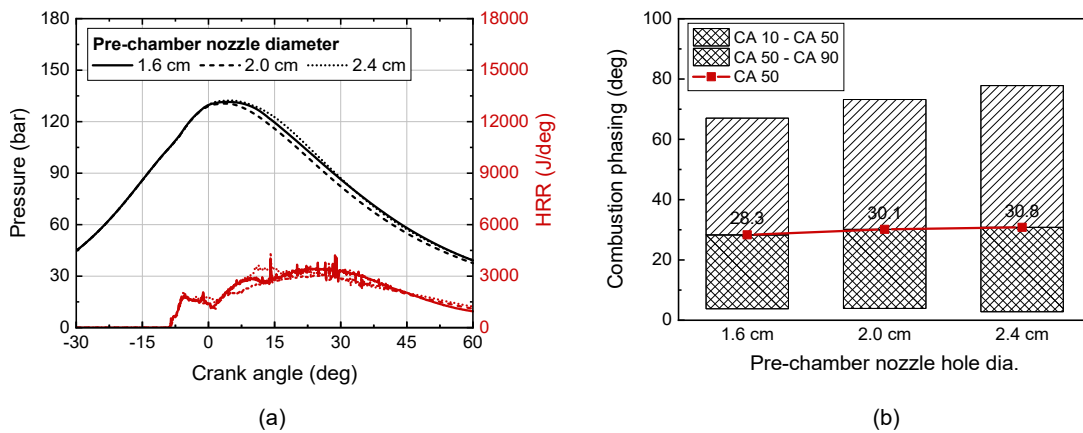


Fig. 12. (a) In-cylinder pressure and heat release rate and (b) combustion phasing based on the pre-chamber nozzle hole diameter in diesel mode operation.

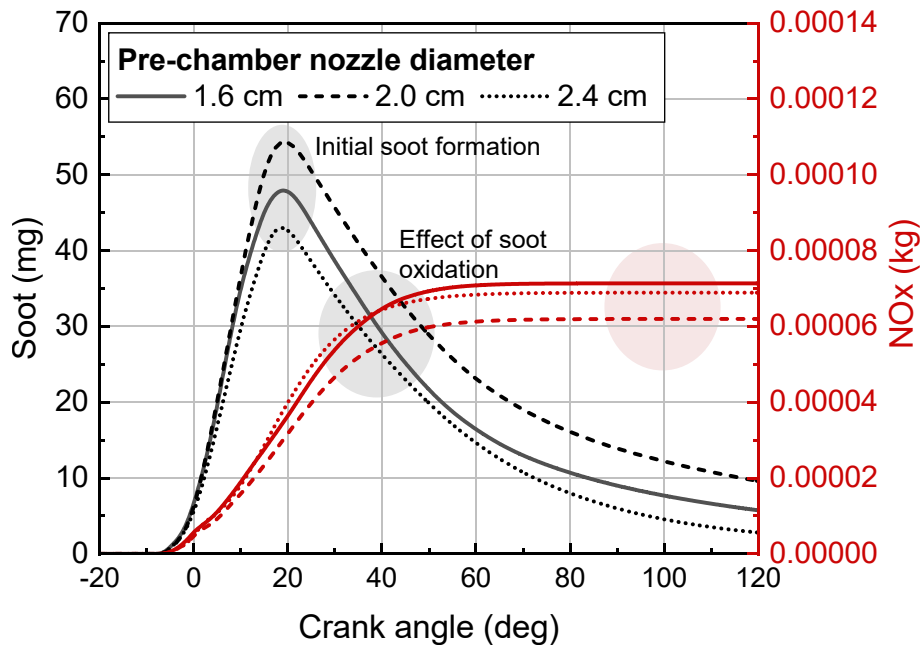


Fig. 13. Soot and NOx history in the combustion chamber based on the pre-chamber nozzle hole diameter in diesel mode operation.

The flame structure in diesel mode operation is similar to the fuel vapor distribution (Fig. 11(b)). As the pre-chamber nozzle hole diameter increased, the jet angle widened, and the jet velocity decreased, reducing the flame diffusion area.

The high-temperature region and flame distribution, which can be used to estimate the combustion temperature, widened as the pre-chamber nozzle hole diameter varied in the following order: 2.4 cm, 1.6 cm, and 2.0 cm during C.A. 0 to C.A. 15 deg. As a result, the peak pressure also increased in the order of 2.4 cm, 1.6 cm, and 2.0 cm, as shown in Fig. 12 (a). The combustion phasing and duration were most affected by the jet velocity. With a larger pre-chamber nozzle hole diameter, the combustion phasing was retarded, and combustion duration lasted longer, as shown in Fig. 12(b).

The initial soot formation during diesel operation is affected by the fuel distribution and temperature. In the fuel rich region, soot formation occurs due to the lack of oxygen. Because the fuel rich region increased based on the nozzle hole diameter in the order of 2.4 cm, 1.6 cm, and 2.0 cm (Fig. 11), the initial soot formation (before C.A. 20 deg) in Fig. 13 follows the same trend. However, because the soot oxidation process takes place in the vicinity of the flame diffusion, the soot oxidation rate

was faster when the pre-chamber nozzle hole diameter was smaller (and the size of the flame diffusion area was larger), as shown by the slope of soot formation trend after C.A. 20 deg. Despite the soot oxidation rate, the amount of soot after combustion increased based on the pre-chamber nozzle hole diameter in the order of 2.4 cm, 1.6 cm, and 2.0 cm.

The production of thermal NOx emissions is expected near the jet periphery, where the temperature is high during combustion. The combustion temperature was higher when the pre-chamber nozzle hole diameter was 2.4 cm than when it was 1.6 cm, but the flame diffusion area was larger when the pre-chamber nozzle hole diameter was 1.6 cm; thus the highest NOx generation occurred with a pre-chamber nozzle hole diameter of 1.6 cm.

As the pre-chamber nozzle hole diameter was increased, a more even flame jet was formed. And combustion duration increased due to the slower flame jet velocity in both dual-fuel and diesel modes. The increase in nozzle hole diameter to 2.4 cm resulted in the NOx reduction and increased IMEP in dual-dual mode and benefited in soot reduction by wider fuel distribution in diesel mode.

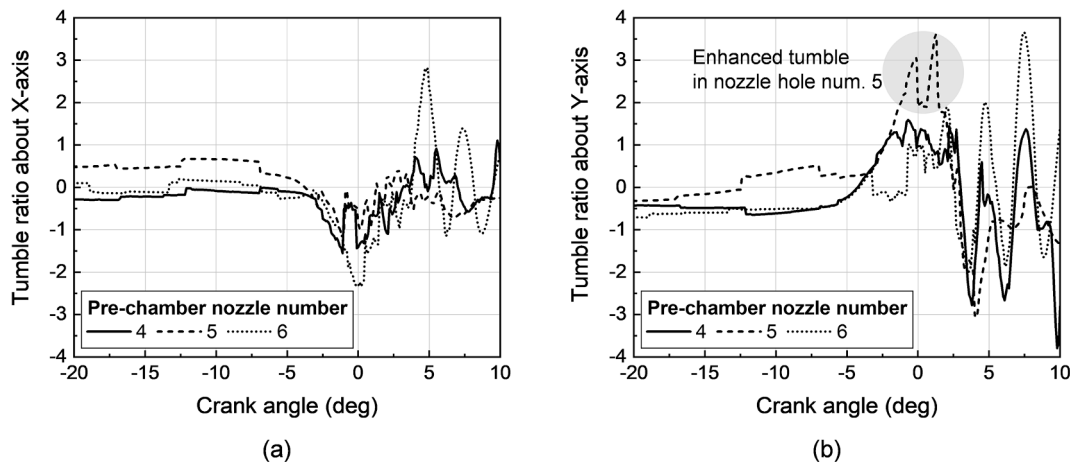


Fig. 14. Tumble ratio in the pre-chamber based on the number of pre-chamber nozzle holes in dual fuel mode: (a) about the X-axis; (b) about the Y-axis.

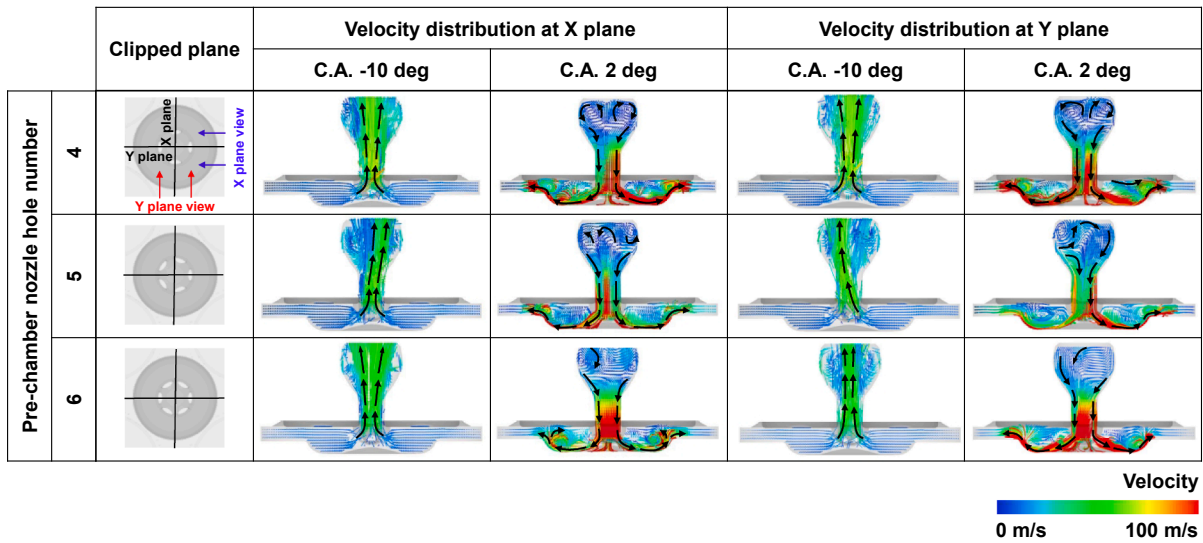


Fig. 15. Velocity distribution based on the number of pre-chamber nozzle holes in dual fuel mode.

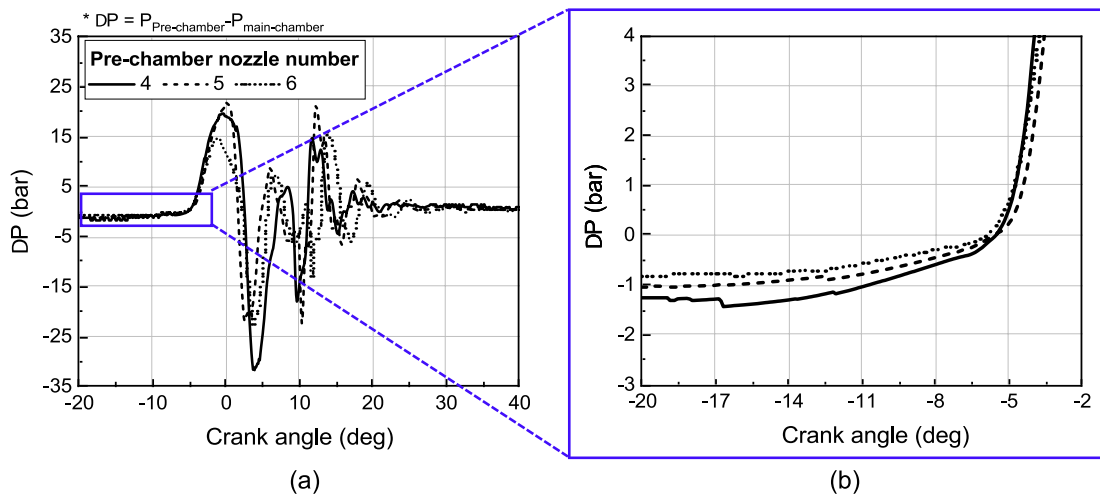


Fig. 16. Pressure difference between the pre-chamber and main chamber based on the number of pre-chamber nozzle holes in dual fuel mode (a) from C.A. -20 deg to C.A. 40 deg, (b) enlarged.

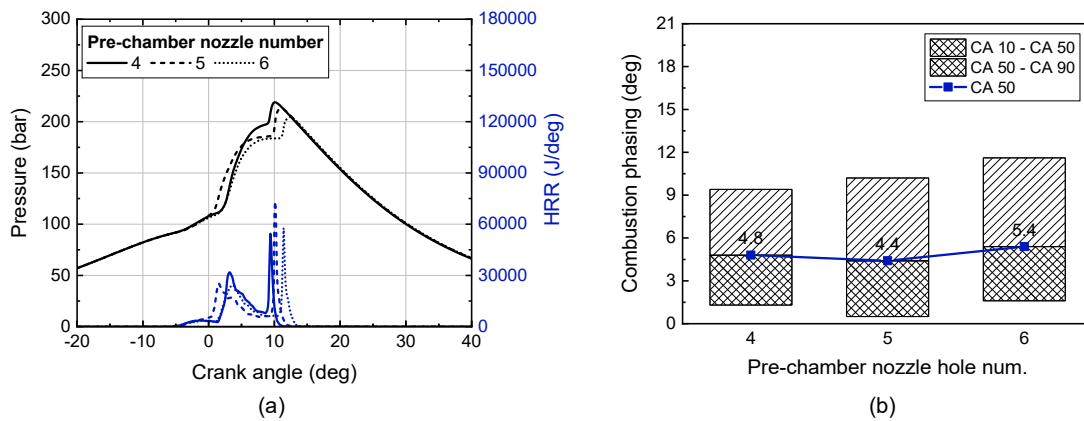


Fig. 17. (a) In-cylinder pressure and heat release rate and (b) combustion phasing based on the number of pre-chamber nozzle holes in dual fuel mode.

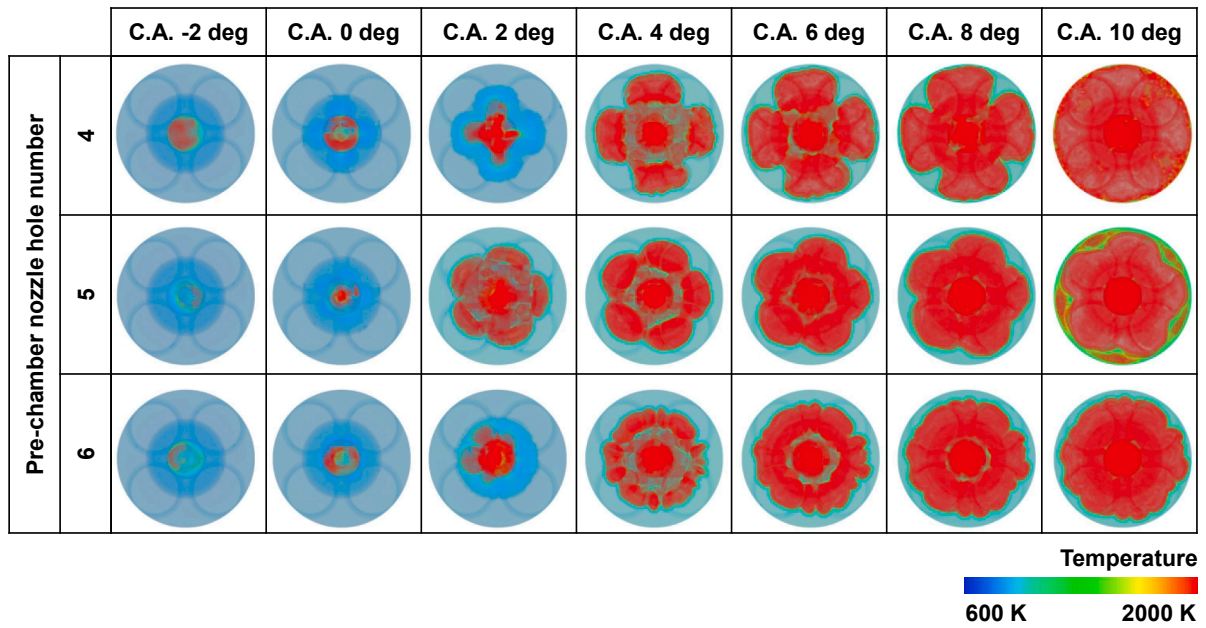


Fig. 18. Flame propagation based on the number of pre-chamber nozzle holes in dual fuel mode.

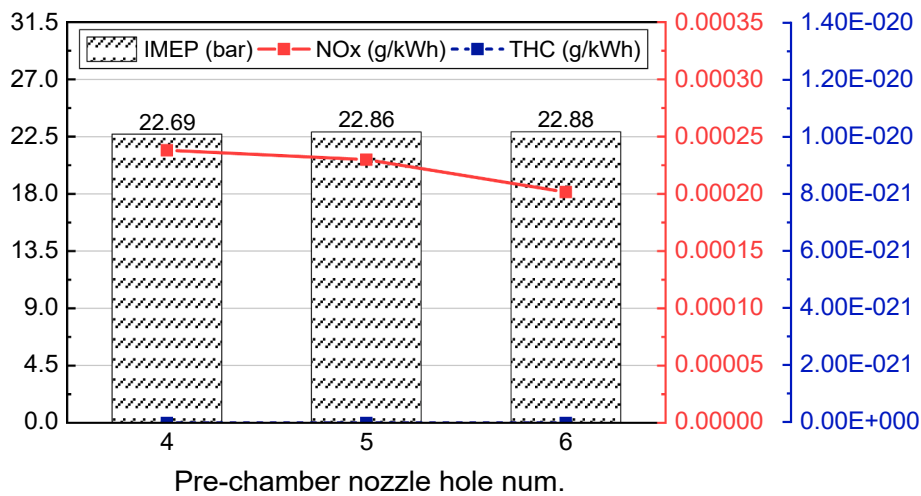


Fig. 19. Gross IMEP and emissions based on the number of pre-chamber nozzle holes in dual fuel mode.

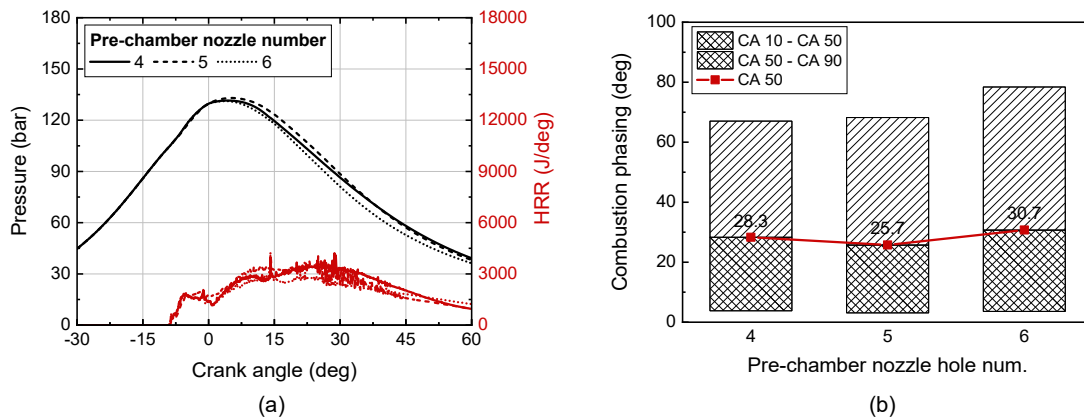


Fig. 20. (a) In-cylinder pressure and heat release rate and (b) combustion phasing based on the number of pre-chamber nozzle holes in diesel mode.

3.3. Influence of the number of pre-chamber nozzle holes

The tumble flow in the pre-chamber can affect the combustion process, particularly the ignition. Strong tumble promotes the atomization and evaporation of injected fuel.

Among the pre-chamber nozzle hole design parameters, the number of holes is closely related to the differences in the tumble ratio. If the number of pre-chamber nozzle holes is odd, the tumble flow could occur in the pre-chamber due to asymmetric flow, as shown in Figs. 14 and 15. In the tumble ratio about the y-axis, the tumble flow was enhanced when the number of pre-chamber nozzle holes was 5 because the pre-chamber nozzle hole was biased with respect to the y-axis.

The pressure difference between the pre-chamber and main chamber increased as the pre-chamber nozzle hole area decreased, as found in the result for different nozzle hole diameters (Fig. 16).

In Fig. 17, the combustion phase is presented for different number of pre-chamber nozzle holes. When the number of nozzle holes was 5, the ignition delay was shorter than those of other cases and was caused by the enhanced tumble flow in the pre-chamber. When the number of nozzle holes increased, the ignition timing was retarded, possibly because the pre-chamber throat volume was not sufficient for mass transport from the pre-chamber to the main chamber when the number of pre-chamber nozzle holes was 6. The peak pressure associated with the jet velocity in dual fuel mode increased as the number of nozzle holes decreased.

Flame propagation is related to the jet velocity from the pre-chamber. As shown in Fig. 18, ignition was fastest when the number of pre-chamber nozzle holes was 5, but flame propagation quickened as the number of pre-chamber nozzle holes decreased.

As the number of pre-chamber nozzle holes increased, the combustion duration also increased. Thus, due to the increase in positive work, the gross IMEP rose to 0.8% as the number of pre-chamber nozzle holes as shown in Fig. 19.

THC formation was dramatically reduced by the pre-chamber combustion system, as explained in Section 3.2.

NOx formation decreased as the number of pre-chamber nozzle holes

increased, and this was related to the peak pressure in dual fuel mode operation. Therefore, the NOx emissions increased with the number of pre-chamber nozzle holes.

In diesel mode operation, as in dual fuel mode, the combustion phasing was slightly advanced when the number of pre-chamber nozzle holes was 5 (Fig. 20(b)). Consequently, near the peak pressure, the high-temperature region was wider and peak cylinder pressure was the highest when the number of pre-chamber nozzle holes was 5 (Fig. 21). However, because the jet velocity is associated with the pre-chamber nozzle area, an increase in the number of nozzle holes correlates with a longer combustion duration.

The initial soot formation is determined by the jet velocity and flame structure. As the pre-chamber nozzle hole number increased, the jet velocity decreased, but the number of jets increased. Thus, increasing the number of nozzle holes was less effective for flame distribution in the radial direction but more effective for wider flame distribution in the angular direction. Fuel vapor distribution can be inferred from the flame distribution. When there were less than 6 pre-chamber nozzle holes, the radial flame propagation was similar, but the angular flame propagation was wider. However, when there were 6 pre-chamber nozzle holes, the jet velocity decreased noticeably, and the fuel vapor was not distributed over as wide an area as in the other conditions. Therefore, the initial soot formation from highest to lowest follows the number of pre-chamber nozzle holes in the order of 5, 4, and 6 (Fig. 22). After C.A. 20 deg, the jet from each nozzle hole merged when there were 5 nozzle holes, and the front flame area was wider when there were 4 nozzle holes compared with 5 holes. Due to the wide flame diffusion area after C.A. 20 deg when the number of pre-chamber nozzle holes was 4, the higher soot oxidation rate produced almost the same amount of soot as when the number of pre-chamber nozzle holes was 5.

A 5-hole pre-chamber design, produced the highest combustion temperature and widest flame diffusion area in the early combustion process, generating the most NOx emissions, followed by nozzle hole numbers 4 and 6 in that order.

In dual-fuel mode, the increase in the number of the pre-chamber nozzle holes had the effect of increasing the IMEP and reducing the

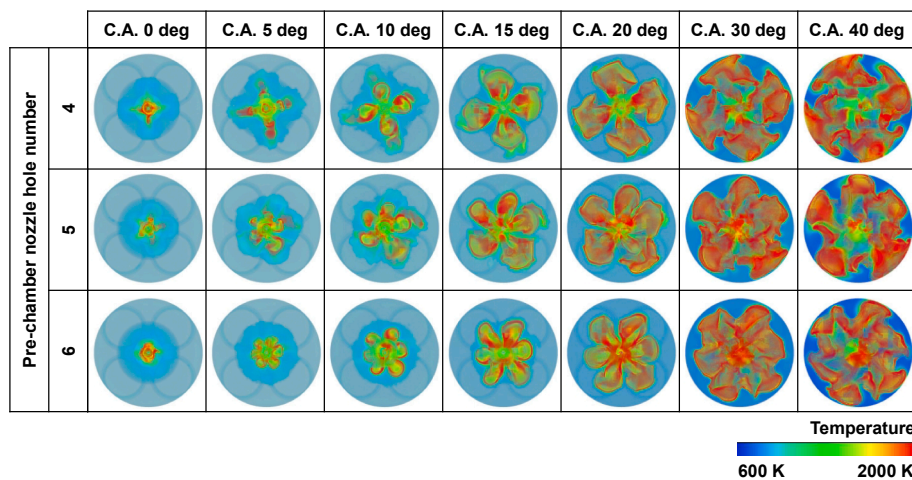


Fig. 21. Flame propagation based on the number of pre-chamber nozzle holes in diesel mode.

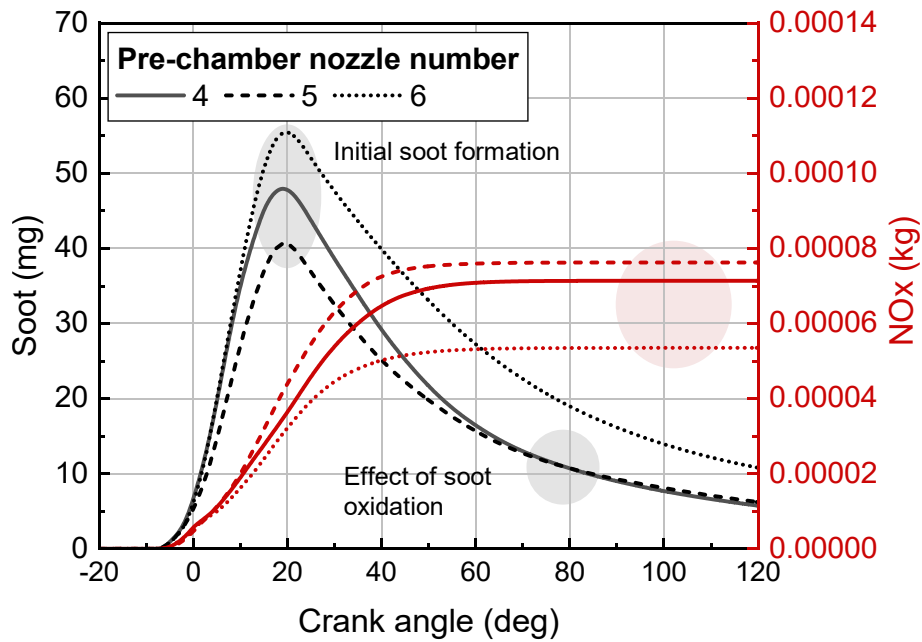


Fig. 22. Soot and NOx history in the combustion chamber based on the number of pre-chamber nozzle holes in diesel mode.

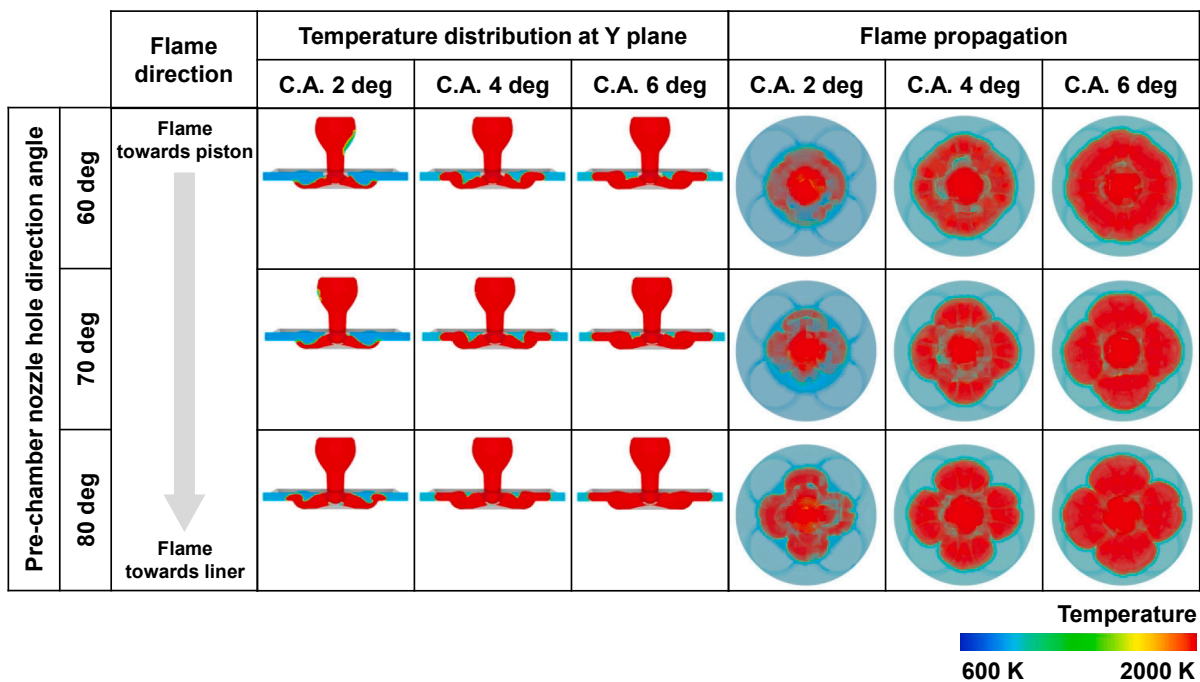


Fig. 23. Flame propagation process based on the pre-chamber nozzle hole direction angle in dual fuel mode.

NO, similarly to the increase in the nozzle hole diameter. However, in diesel mode, there was a noticeable decrease in jet velocity from nozzle hole number of 6 due to limited throat area, which adversely affected soot formation.

3.4. Influence of the pre-chamber nozzle hole angle

The relationship between the jet from the pre-chamber nozzle and the piston is an important factor in combustion performance. Thus, the influence of pre-chamber nozzle hole angle was investigated.

Changing the pre-chamber nozzle hole direction angle alters the targeting of the jet from the pre-chamber. As the direction angle

decreases, the jet targets the piston. If the jet is ejected toward the piston, flame mixing occurs through jet impingement and sliding in the piston bowl. Thus, as the jet direction goes toward the piston, the flame mixes in the piston bowl and is propagated in a more united form, as shown in Fig. 23. Through this additional process, the flame speed decreased when the jet was targeted toward the piston in dual fuel mode operation.

As the flame propagation speed decreased with decreasing nozzle direction angle, the combustion duration lasted longer. As a result, the peak pressure decreased and the combustion phasing was retarded (Fig. 24).

The gross IMEP remained almost the same as the nozzle hole

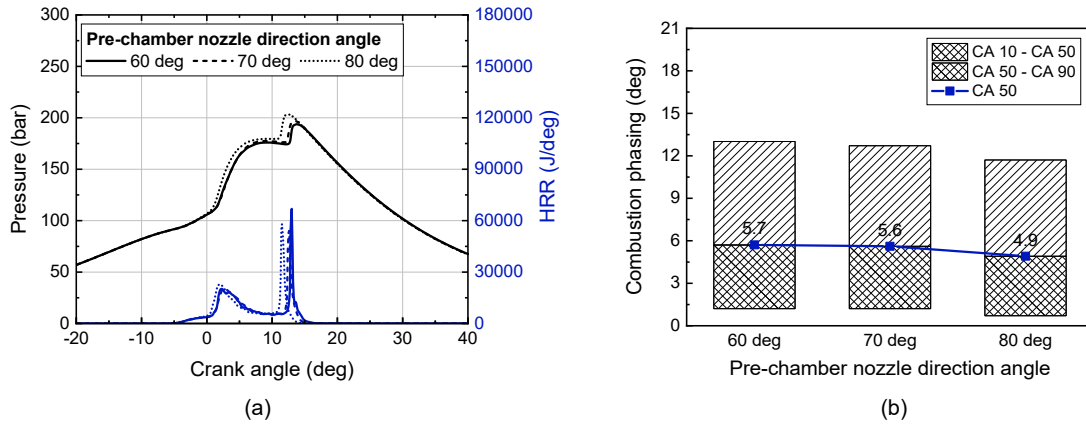


Fig. 24. (a) In-cylinder pressure and heat release rate and (b) combustion phasing based on the pre-chamber nozzle hole direction angle in dual fuel mode.

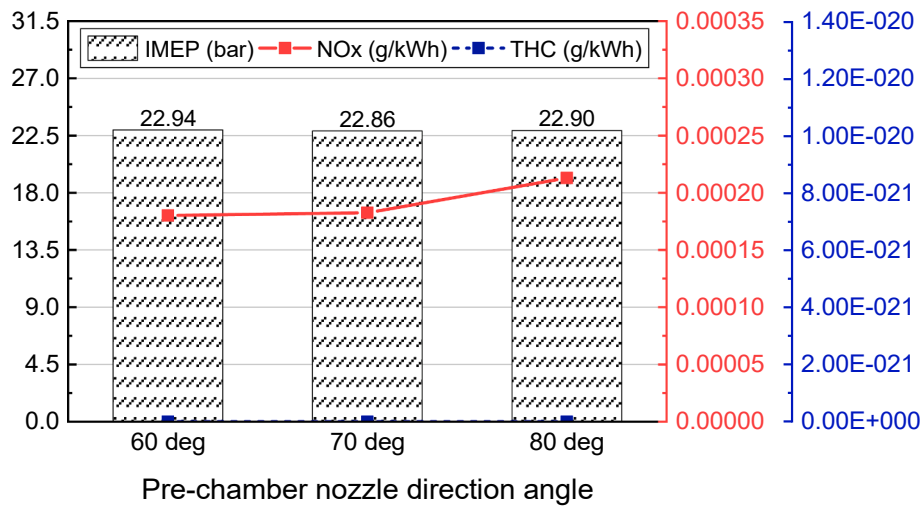


Fig. 25. Gross IMEP and emissions based on the pre-chamber nozzle hole direction angle in dual fuel mode operation.

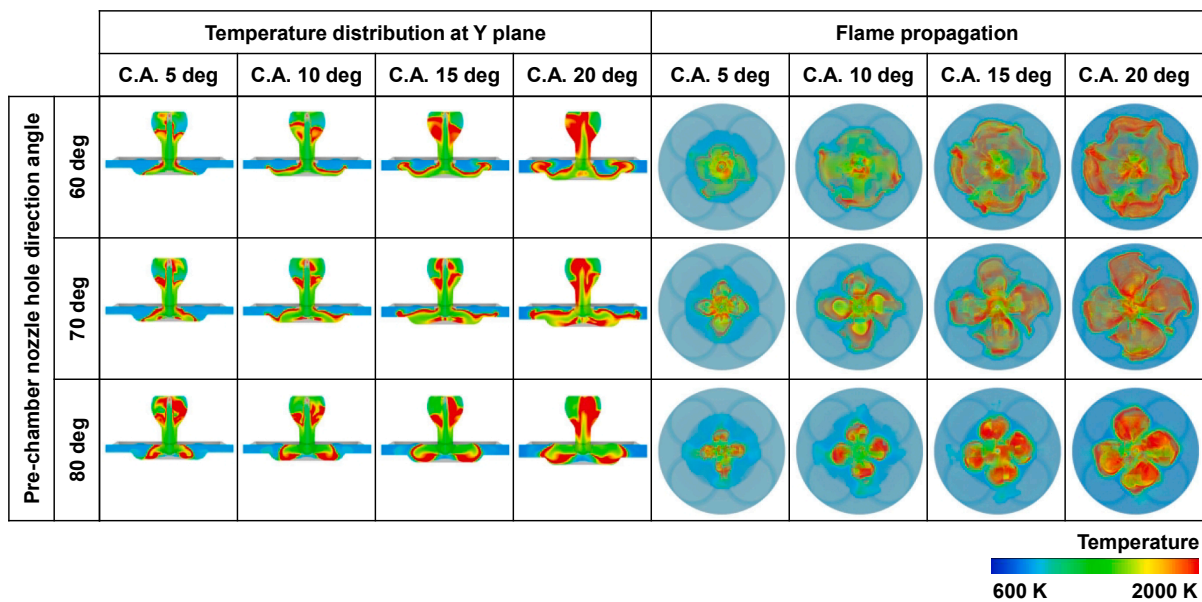


Fig. 26. Flame propagation process based on the pre-chamber nozzle hole direction angle in diesel mode operation.

Table 5
Integrated heat release rates with different nozzle hole direction angles.

Pre-chamber nozzle direction angle	Integrated heat release rate
60 deg	189410 J
70 deg	181520 J
80 deg	178422 J

direction angle changed. With the increase in the nozzle hole direction angle, the NOx emissions increased because of the higher combustion temperature. Very little THC was produced in the pre-chamber combustion system. See (Fig. 25).

In diesel mode operation, combustion occurs in the region containing the diesel fuel vapor from the pre-chamber; thus, the combustion progress depends on the diesel fuel vapor propagation. As shown in Fig. 26, the flame propagation with various pre-chamber nozzle targets has different trends from those in dual fuel mode operation. In diesel mode, the combustion duration lasted much longer than in dual fuel mode. Therefore, the momentum of the jet was weakened by the decreasing pressure difference between the pre-chamber and main chamber during C.A. 15 deg to C.A. 30 deg. Then, the piston’s rapid downward movement pulled the fuel out of the pre-chamber, producing another momentum for propagation during C.A. 15 deg to C.A. 30 deg. When the nozzle hole direction was directed toward the piston, the jet containing the diesel fuel vapor impacted the piston bowl and then moved along it. However, when the nozzle hole direction was directed toward the liner, the jet had no way to obtain additional momentum. Thus, the flame propagated more quickly when the nozzle hole was directed toward the piston.

The fast and even flame propagation when the nozzle hole direction angle was 60 deg produced the highest integrated heat release rate, which represents combustion efficiency (Table 5). Because the combustion phasing is calculated based on the integrated heat release rate, the combustion duration was the longest and the most delayed for this case (Fig. 27).

As inferred from the flame structure, the initial soot formation decreased as the nozzle hole direction angle decreased, as shown in Fig. 28. This is because the more wrinkled flame front area when the nozzle hole direction was 70 deg or 60 deg provided more soot oxidation area, as shown in the temperature distribution and flame in Fig. 26. Therefore, soot formation decreased when the pre-chamber nozzle hole direction angle decreased.

The peak pressure remained almost the same for all direction angles, but the front area of the flame diffusion decreased with the pre-chamber nozzle hole direction angle in the order of 70 deg, 60 deg, and 80 deg during flame propagation. Thermal NOx formed in this area; thus, NOx production decreased for the same direction angle order.

As the pre-chamber nozzle hole direction was toward the piston

bowl, the flame spreads in a more united form due to the effect of flame mixing. As a result, it had a positive effect on the efficiency and NOx of dual-fuel mode, and soot of diesel mode.

3.5. Effect of a pre-chamber combustion system

To evaluate the efficiency and emissions of the pre-chamber combustion system compared with the conventional engine system, the normalized results regarding efficiency and emissions are represented in Table 6.

Table 6 presents the gross IMEP, NOx, and THC that were normalized based on data for a conventional engine without a pre-chamber in dual-fuel operation mode. By applying a pre-chamber combustion system, the gross IMEP increased to a maximum of 0.8% compared with the conventional engine. Due to the rapid and even flame spread, the amount of THC production was significantly reduced in the pre-chamber combustion system. However, the high peak combustion pressure due to the short combustion period resulted in increased NOx production, indicating a trade-off with THC formation. These results indicate that the optimal design includes a pre-chamber nozzle hole diameter of 2.4 cm, 4 pre-chamber nozzle holes, and a pre-chamber nozzle hole direction angle of 60 deg.

In diesel mode operation, the NOx production was reduced due to the prolonged combustion period (Table 7). However, the soot formation increased compared with that of the conventional diesel engine. This was because a fuel-rich region was formed as a large amount of diesel fuel was injected into the pre-chamber having a relatively small volume compared with the main combustion chamber. Considering the soot and NOx production, a pre-chamber nozzle design with a hole size of 2.4 cm, 4 holes, and a nozzle hole direction of 60 deg demonstrated the best results also in diesel mode.

Applying the pre-chamber combustion system to the heavy-duty engine increased the engine efficiency by up to 0.8% and decreased the methane slip, resulting in a significant reduction in THC in dual-fuel mode. In diesel mode, when the optimal pre-chamber design was applied, the NOx production decreased by 50% compared with that of the conventional engine. However, when pre-chamber was applied, NOx production increased in dual-fuel mode and soot production increased in diesel mode. Comparing the results of dual-fuel mode and diesel mode, it is considered that there will be a condition in which NOx and soot do not deteriorate while maintaining the advantages of current pre-chamber application results depending on the ratio of methane and diesel. Therefore, to solve these problems and practically apply pre-chamber to a heavy-duty engine, additional research on engine operation strategies involving, for example, the ratio of methane fuel and diesel fuel and micro pilot diesel injection timing is required.

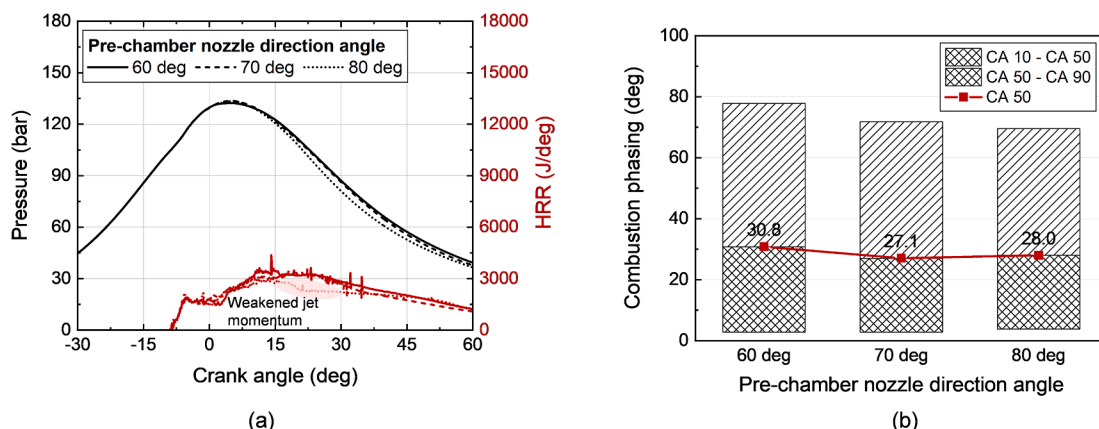


Fig. 27. (a) In-cylinder pressure and heat release rate and (b) combustion phasing based on the pre-chamber nozzle hole direction angle in diesel mode operation.

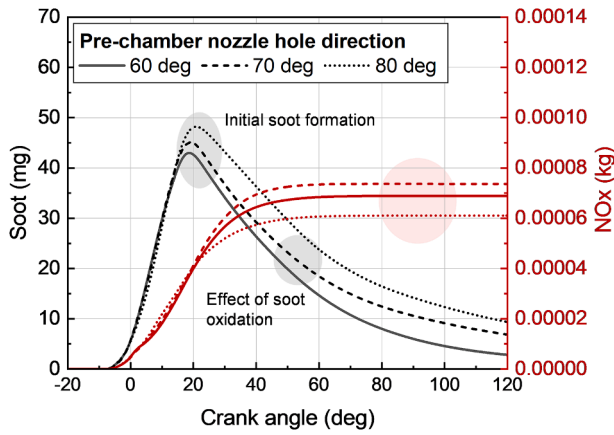


Fig. 28. Soot and NOx history in the combustion chamber based on the pre-chamber nozzle hole direction angle in diesel mode operation.

Table 6 Normalized Gross IMEP, NOx, and THC based on data for a conventional engine w/o pre-chamber in dual-fuel mode operation.

Normalized based on data w/o pre-chamber			IMEP	NOx	THC
Pre-chamber nozzle hole dia.	Pre-chamber nozzle hole num.	Pre-chamber nozzle direction angle			
1.6 cm	4	60 deg	0.997	6.679	1.1E-4
2.0 cm			1.007	5.841	1.4E-4
2.4 cm			1.008	5.053	1.3E-4
1.6 cm	4	60 deg	0.997	6.679	1.1E-4
	5		1.005	6.447	1.2E-4
	6		1.006	5.655	1.1E-4
2.4 cm	4	60 deg	1.008	5.053	1.3E-4
		70 deg	1.005	5.119	1.2E-4
		80 deg	1.007	5.715	1.1E-4

4. Conclusion

In this study, we conducted CFD analyses to investigate the combustion process of a pre-chamber system and understand how pre-chamber design parameters influenced engine efficiency and emissions in both dual fuel and diesel-only operation modes. The results are as follows.

1. In pre-chamber combustion systems, the combustion has occurred in three stages. It was clearly distinguished by in-cylinder heat release rate during combustion. In dual-fuel mode, stages were shown in order of combustion in pre-chamber, ejection of flame jet and its propagation, and fast flame propagation by wide flame area. On the other hand, in diesel mode, the combustion occurred in the sequence of combustion in pre-chamber, ejection of jet and mixing controlled combustion, and late burning from the rest of fuel. The flame diffusion area which affected the soot and NOx formation was determined by the shape of ejected fuel to the main chamber through the nozzles in pre-chamber.
2. In dual fuel mode operation, the gross IMEP increased by up to 1.1% as the pre-chamber nozzle hole diameter increased from 1.6 cm to 2.4 cm as a result of the longer combustion duration after TDC

Table 7

Normalized Soot and NOx based on data for a conventional engine w/o pre-chamber in diesel mode operation.

Normalized based on data w/o pre-chamber			Soot	NOx
Pre-chamber nozzle hole dia.	Pre-chamber nozzle hole num.	Pre-chamber nozzle direction angle		
1.6 cm	4	60 deg	78.0	0.52
2.0 cm			130.3	0.45
2.4 cm			38.2	0.50
1.6 cm	4	60 deg	78.0	0.52
	5		84.4	0.55
	6		146.5	0.39
2.4 cm	4	60 deg	38.2	0.50
		70 deg	92.9	0.53
		80 deg	126.9	0.44

induced more positive work. A peak pressure decrement led to reduced NOx emissions with increasing nozzle hole diameter. In diesel mode, soot production was the lowest and the most even fuel distribution was produced in the main chamber when the nozzle hole diameter was 2.4 cm. NOx emissions were the highest when the hole diameter was 1.6 cm due to the flame diffusion area.

3. When the number of nozzle holes was 5, the ignition delay was shortened due to the enhanced tumble. In dual fuel mode operation, the gross IMEP increased up to 0.8% as the hole number varied from 4 to 6. Furthermore, the decreased peak pressure caused by the slower flame jet velocity as the hole number increased resulted in reduced NOx formation. In diesel mode operation, when the number of nozzle holes was 6, the slow flame jet interrupted the diesel fuel supply to the main chamber, causing the highest production of soot. NOx formation was highest when the nozzle hole number was 5 because of the high peak pressure from the combustion phasing.
4. Changing the pre-chamber nozzle hole direction angle changed the flame structure. In diesel mode operation, angling the nozzle direction toward the piston effectively enhanced combustion efficiency and reduced soot formation.
5. When comprehensively evaluating in dual-fuel and diesel modes, the most optimal results were obtained with a pre-chamber nozzle hole diameter of 2.4 cm, 4 nozzle holes, and a direction angle of 60 deg. As compared with a conventional heavy-duty engine, the engine efficiency was increased by up to 0.8% and THC was significantly reduced in dual-fuel mode with a pre-chamber combustion system. The NOx production decreased by 50% in diesel mode. However, the deterioration of NOx in dual-fuel mode and soot in diesel mode occurred. Therefore, future research on engine operating strategies involving the ratio of methane and diesel fuel, as well as injection strategies is required.

CRediT authorship contribution statement

Jisoo Shin: Writing – original draft, Conceptualization, Methodology, Investigation. Jonghui Choi: Investigation. Jaeyeob Seo: Conceptualization, Methodology. Sungwook Park: Writing – review & editing, Supervision.

Declaration of Competing Interest

The authors declare that they have no known competing financial interests or personal relationships that could have appeared to influence the work reported in this paper.

Acknowledgments

This work was supported by BK21 FOUR program from National Research Foundation and Mistry of Education.

References

- [1] Johnson T, Joshi A. Review of vehicle engine efficiency and emissions. *SAE Int J Engines* 2018;11:1307–30. <https://doi.org/10.2307/26649163>.
- [2] Reitz RD, Duraisamy G. Review of high efficiency and clean reactivity controlled compression ignition (RCCI) combustion in internal combustion engines. *Prog Energy Combust Sci* 2015;46:12–71. <https://doi.org/10.1016/j.pecc.2014.05.003>.
- [3] Saiteja P, Ashok B. A critical insight review on homogeneous charge compression ignition engine characteristics powered by biofuels. *Fuel* 2021;285:119202.
- [4] Ashok B, Ashok SD, Kumar CR. LPG diesel dual fuel engine—A critical review. *Alexandria Eng J* 2015;54:105–26.
- [5] Tanoue K, Kimura T, Jimoto T, Hashimoto J, Moriyoshi Y. Study of prechamber combustion characteristics in a rapid compression and expansion machine. *Appl Therm Eng* 2017;115:64–71. <https://doi.org/10.1016/j.applthermaleng.2016.12.079>.
- [6] Regueiro JF. The case for new divided-chamber diesel combustion systems: part two: critical analysis of, and solutions for. *Swirl-Prechamber Engines*: SAE transactions; 2001. p. 240–61.
- [7] Nishida K, Hiroyasu H, Matsuoka T, Yamauchi H. Characterization of combustion processes in the prechamber and main chamber of an indirect injection Diesel engine by high-speed photography. *SAE Trans* 1986:745–69.
- [8] Salahi MM, Esfahanian V, Ghareghani A, Mirsalim M. Investigating the reactivity controlled compression ignition (RCCI) combustion strategy in a natural gas/diesel fueled engine with a pre-chamber. *Energy Convers Manage* 2017;132:40–53. <https://doi.org/10.1016/j.enconman.2016.11.019>.
- [9] Esfahanian V, Salahi MM, Ghareghani A, Mirsalim M. Extending the lean operating range of a premixed charged compression ignition natural gas engine using a pre-chamber. *Energy* 2017;119:1181–94. <https://doi.org/10.1016/j.energy.2016.11.071>.
- [10] Huang J, Lin L, Wang Y, Qin J, Roskilly AP, Li L, et al. Experimental study of the performance and emission characteristics of diesel engine using direct and indirect injection systems and different fuels. *Fuel Process Technol* 2011;92:1380–6. <https://doi.org/10.1016/j.fuproc.2011.03.001>.
- [11] Iwazaki K, Amagai K, Arai M. Improvement of fuel economy of an indirect injection (IDI) diesel engine with two-stage injection. *Energy* 2005;30(2-4):447–59. <https://doi.org/10.1016/j.energy.2004.05.009>.
- [12] Gentz G, Thelen B, Gholamisheeri M, Litke P, Brown A, Hoke J, et al. A study of the influence of orifice diameter on a turbulent jet ignition system through combustion visualization and performance characterization in a rapid compression machine. *Appl Therm Eng* 2015;81:399–411. <https://doi.org/10.1016/j.applthermaleng.2015.02.026>.
- [13] Shah A, Tunestal P, Johansson B. Effect of pre-chamber volume and nozzle diameter on pre-chamber ignition in heavy duty natural gas engines, in. *SAE Technical Paper* 2015.
- [14] Yakhot V, Orszag SA. Renormalization group analysis of turbulence. I. Basic theory. *J Sci Comput* 1986;1(1):3–51.
- [15] Yakhot V, Orszag SA, Thangam S, Gatski TB, Speziale CG. Development of turbulence models for shear flows by a double expansion technique, *Physics of Fluids A. Fluid Dyn* 1992;4(7):1510–20.
- [16] Beale J, Reitz R. Modeling spray atomization with the Kelvin-Helmoltz/Rayleigh-Taylor hybrid model., in. *At Sprays* 1999;9:623–50.
- [17] V. Golovitchev, Chalmers University of Technology, Gothenburg, Sweden, <http://www.tfd.chalmers.se/%7Evaleri/MECH.html>, 2000. (accessed September 01 2021).
- [18] Peters N, editor. *Turbulent Combustion*. Cambridge University Press; 2000.
- [19] J. Ewald, N. Peters, A level set based flamelet model for the prediction of combustion in spark ignition engines, in: 15th International Multidimensional Engine Modeling User's Group Meeting, Detroit, MI, 2005.
- [20] Gülder ÖL. Correlations of laminar combustion data for alternative SI engine fuels, in. *SAE Technical Paper* 1984.
- [21] Heywood JB. *Internal combustion engine fundamentals*. McGraw-Hill Education; 2018.
- [22] Hiroyasu H, Kadota T. Models for combustion and formation of nitric oxide and soot in direct injection diesel engines. *SAE Trans* 1976:513–26.
- [23] Papagiannakis R, Hountalas D. Experimental investigation concerning the effect of natural gas percentage on performance and emissions of a DI dual fuel diesel engine. *Appl Therm Eng* 2003;23:353–65. [https://doi.org/10.1016/S1359-4311\(02\)00187-4](https://doi.org/10.1016/S1359-4311(02)00187-4).
- [24] Wei L, Geng P. A review on natural gas/diesel dual fuel combustion, emissions and performance. *Fuel Process Technol* 2016;142:264–78. <https://doi.org/10.1016/j.fuproc.2015.09.018>.
- [25] Azimov U, Tomita E, Kawahara N, Harada Y. Premixed mixture ignition in the end-gas region (PREMIER) combustion in a natural gas dual-fuel engine: operating range and exhaust emissions. *Int J Engine Res* 2011;12:484–97.
- [26] Heywood J. *Internal combustion engine fundamentals*. New York: McGraw-Hill; 1988.
- [27] Dec JE. A conceptual model of DI diesel combustion based on laser-sheet imaging. *SAE Trans* 1997:1319–48.
- [28] Dec JE, Coy EB. OH radical imaging in a DI diesel engine and the structure of the early diffusion flame. *SAE Trans* 1996:1127–48.
- [29] Ma F, Wang Y, Wang J, Ding S, Wang Y, Zhao S. Effects of combustion phasing, combustion duration, and their cyclic variations on spark-ignition (SI) engine efficiency. *Energy Fuels* 2008;22:3022–8. <https://doi.org/10.1021/ef8003027>.
- [30] Caton JA. Combustion phasing for maximum efficiency for conventional and high efficiency engines. *Energy Convers Manage* 2014;77:564–76. <https://doi.org/10.1016/j.enconman.2013.09.060>.